



Pedestrian headways – Reflection of territorial social forces



Milan Krbálek^{a,*}, Pavel Hrabák^b, Marek Bukáček^a

^a Department of Mathematics, Faculty of Nuclear Sciences and Physical Engineering, Czech Technical University in Prague, Prague, Czech Republic

^b Faculty of Civil Engineering, Brno University of Technology, Brno, Czech Republic

HIGHLIGHTS

- We introduce two functional candidates for the headway distribution detected in pedestrian crowds.
- We quantitatively estimate repulsion forces for the social force model.
- We estimate a level of stochastic resistivity in walkers groups.
- Empirical/experimental data samples are subjected to an analysis of the statistical rigidity.
- We compare statistical properties of microstructure between pedestrian and vehicular samples.

ARTICLE INFO

Article history:

Received 1 October 2016

Received in revised form 25 June 2017

Available online 14 August 2017

Keywords:

Pedestrian dynamics

Microstructure of a crowd

Headway distribution

ABSTRACT

The aim of the article is to give a more detailed insight into territorial social forces acting between pedestrians by means of headway distribution and spectral rigidity. Probabilistic distribution of time headways between consecutive pedestrians is studied theoretically and experimentally. Several original experiments/empirical observations are presented and compared to data obtained from previously published experiments. The study is restricted to an unidirectional one-lane motion where overtaking is forbidden.

The main stress is put on natural choices of mutual interaction represented by logarithmic and hyperbolic potentials leading to gamma and generalized inverse Gaussian distribution respectively. We show that the time headway distribution does not sufficiently reflect the differences between such distributions. The tools related to spectral rigidity and compressibility are chosen instead so as to predict the territorial social forces more accurately. Surprisingly, pedestrian flow seems to show a higher level of synchronization (lower compressibility) than vehicular flow.

© 2017 Elsevier B.V. All rights reserved.

1. Motivation and goals

Pedestrian crowds display a wide variety of dynamic features which are of great interest for scientists. Currently, the general qualitative properties of pedestrian flow are relatively well researched (see Refs. [1–3] for general overview). However, contrary to the physics of traffic, quantitative description of mutual interactions among pedestrians is still considerably vague. Although in recent years many experiments have been arranged, their quantitative evaluations face a number of technical problems (i.e. digital image processing, automatic detection of pedestrian trajectories, insufficiently large samples of data, mathematically informal/inconsistent definitions of basic quantities, etc.). These problems significantly complicate

* Corresponding author.

E-mail address: milan.krbalek@jfifi.cvut.cz (M. Krbálek).

the way to a more detailed insight into pedestrian dynamics. On the other hand, this field is rapidly advancing, which allows answering more complex questions about social forces acting inside groups of moving humans.

Generally, the main goal of this article is to present (and evaluate) original experiments resulting in detection of the so-called time headway distribution (probability density for the time gap measured between two successive walkers when passing a given point in a corridor/aisle) and find a theoretical elucidation for its course. The headway distributions detected for various experimental/empirical systems may then lead (similar to [4,5]) to a quantitative adjustment of interaction forces in the social force models. More specifically, the main objectives of this work can be established as follows.

- We aim to report on a series of original pedestrian experiments arranged for revealing quantitative properties of microstructure in one-dimensional pedestrians traffic. Besides headway distributions we will also analyze advanced statistical properties (e.g. statistical rigidity [6]).
- We aim to confirm/reject the hypothesis that statistical properties of pedestrian flows are similar to those detected in vehicular traffic (see [7–9,1]). Furthermore, we aim to compare levels of synchronization in both systems.
- We intend to introduce relevant mathematical predictions for experimental/empirical headway distributions and the associated statistical rigidity (similar to [10]).
- Using mathematical estimations for headway distribution and analytically derived rigidity we intend to improve the existing knowledge of distance dependence of interaction forces acting between pedestrians (published in [11]).

2. Introduction

In typical social force based models (like in [12,13]) the acceleration equation includes four basic types of forces: (1) acceleration term describing tendency to reach the desired area as soon as possible (with a certain desired velocity); (2) interaction term describing the psychological tendency of two pedestrians keeping sufficient distance between one another; (3) repulsive term describing interaction with borders/walls/obstacles; (4) fluctuation term arising from accidental or deliberate deviations from the usual rules of motion. As evident, global detection and validation of all acceleration/deceleration factors is not realistic because of the complexity of the system investigated. For this reason, it is necessary to restrict the issue of crowd dynamics to minor tasks only. One of the possibilities to do so is to formulate a simplified version of pedestrian flow where some of the above-mentioned effects are suppressed. Therefore, for the purpose of this paper we take into consideration unidirectional one-lane flows of walkers whose movement can be classified as non-panic, i.e. comfortable and safe movement of people through a narrow corridor. Such restriction is convenient and, at the same time, essential for completion of the afore-mentioned tasks. Thus, proceeding in a similar way to [3,11,14,15] we have performed several experiments (see Section 4) suitable for revealing statistical distributions of time gaps between walkers.

Automatic or semi-automatic processing of video recordings from the experiments (see e.g. [16]) allows detecting the times of individual pedestrian's passing through the observed cross-section. Let us denote by t_j the passage time of j th pedestrian, $j \in \{0, 1, \dots, N\}$. Then we can define the re-scaled time headway as

$$\tau_j = \frac{N(t_j - t_{j-1})}{t_N - t_0}. \quad (1)$$

Thus we obtain a set $\{\tau_j : j = 1, 2, \dots, N\}$ of all successive (re-scaled) headways with an average value equal to one. This set represents the fundamental subject of our investigations. The scaling procedure is introduced for several obvious reasons. Firstly, the re-scaling to the unit mean headway allows to compare data from various sources/countries/situations without any substantial loss of generality. Secondly, such a procedure is well established in the physics of traffic (e.g. [6,8]), where it is applied to analytical predictions of vehicular microstructure. Thirdly, it is well known from Random Matrix Theory [17] that the scaling procedure (as a significant part of the general procedure called *unfolding* – see [18]) reveals a universality in the spectra of random matrices. Besides others, such approach has been useful in finding a relation between vehicular samples (or public transport samples) and certain classes of random matrices (see [18–21]).

Choosing an appropriate division of a time axis Δ_τ , one can define the empirical/experimental histogram function

$$H(\tau|\Delta_\tau) := \frac{|\{j : \lfloor \tau/\Delta_\tau \rfloor \leq \tau_j/\Delta_\tau < \lceil \tau/\Delta_\tau \rceil\}|}{N}, \quad (2)$$

as an estimation of the probability density function of the time headway distribution. Here $\lfloor \cdot \rfloor$, $\lceil \cdot \rceil$ stand for the floor/ceiling functions respectively, and $|\cdot|$ stands for cardinality. For greater clarity, if necessary, the graphical representation of the histogram function (step function) may be replaced by a scatter chart depicting point-set $\{(\Delta_\tau/2 + k\Delta_\tau; H(\Delta_\tau/2 + k\Delta_\tau|\Delta_\tau)) \in \mathbf{R}^2 : k = 0, 1, \dots\}$.

For unidirectional flows in a narrower corridor (where overtaking is improbable/prohibited) one can expect that the most decisive dynamic factor is the territorial social force reflecting a repulsive effect between *private spheres* of two persons. Such territorial effect (see [22]) can be expressed by a mathematical formula/graph (similar to [3,11]), which is the desired output. Since these territorial forces influence decision-making of walkers, their action must be reflected in the headway distribution. Thus, there exists a direct link between the territorial forces and microstructure of pedestrian crowds. This link is definitely intricate, however, a simplified conception can be obtained (in analogy with [4,5,8]) by the following considerations. In one-dimensional flows private spheres are reduced to *private intervals*, which allows to introduce repulsive forces in a simplified

form $f_{j,k}(s_{j,k})$, where $s_{j,k}$ is the distance between walkers (j th and k th). Although this force (measuring how j th person is influenced by k th person) is not known, some of its properties are expectable: (1) $f(0_+) = +\infty$ due to impossibility of overtaking; (2) there exists $s_0 > 0$ so that for all $s > s_0$ it holds that $f(s) = 0$; [alternatively: (2) $\lim_{s \rightarrow 0_+} f(s) = 0$]; (3) in all cases $f_{j,k}(s) = 0$ for all s and all $k = j, j + 1, j + 2, \dots$; (4) in all cases $f_{j,j-1}(s) \gg f_{j,j-2}(s)$ for all s . Thus, such behavior can be classified as short-ranged because the dominant force is initiated by a predecessor. For correctness, let us remark that all these considerations are valid for the afore-mentioned one-lane unidirectional scenarios only. Velocity differences are not considered. For purposes of analytical derivations (instead of individual formulas for every $f_{j,k}(s)$) we use the common force description: $f(s)$. For taking into account accidental deviations we introduce a stochastic variant of the ensemble, where the level of stochasticity is regulated by the coefficient of resistivity $\beta \geq 0$. This parameter reflects the global state of the system determined by the density of walkers, corridor width, initial arrangement of walkers, and so on. Such a simplistic approach brings a significant profit: analytical derivation of associated headway distribution. As proven in [4,5] and generalized in [6,23] the headway distribution (abbreviated by THD) of such an ensemble reads

$$\varphi(\tau|\beta) = A\Theta(\tau)e^{-\beta\varphi(\tau)}e^{-D\tau}, \quad (3)$$

where

$$\varphi(\tau) = -\int_0^\tau f(s) ds, \quad (4)$$

$\Theta(x)$ is Heaviside's unit-step function, and A, D are constants for proper normalization and scaling. It is worth noting that although the one-parametric probability density (3) has been derived for thermal equilibrium of particle gas with symmetrical interactions the papers [8,9,24] justified the possibility of approximating some driven many-particle systems by Hamiltonian systems. Indeed, the paper [24] proves that analytical gap distributions like (3) can be derived from a simple non-isotropic thermodynamic model of driven particles.

Thus, detection of empirical/experimental headways and relevant statistical estimations of associated THD may lead to calibration of the force model used. This will be the subject of the following sections. The importance of the knowledge of THD for the model calibration is summarized in article [25]. The time headway distribution in pedestrian bottleneck flow has been studied in [10] and [26]. However, the stress of these studies was given to the estimation of statistical model parameters. Here it is worth noting that the time headways are closely related to the flow, namely, flow is the inverse of the THD mean. Since the flow and its dependence on bottleneck width and other aspects has been well studied recently (see e.g. [27,28]), we focus on the above mentioned scaled THD, in which the flow-related information is suppressed in order to highlight the aspects of repulsive interaction reflected in the headway distribution.

3. Principal attribute of socio-physical headway distributions

Alternatively, one can view the detection of headway distributions from a more theoretical perspective. Omitting the detailed empirical background or theoretical models of pedestrian flows we now aim to reveal functional restrictions resulting from a purely mathematical point of view, i.e. the goal is to detect certain principal attributes of socio-physical headway distributions. From such a perspective we are dealing with an ensemble of particles whose mutual interactions are short/middle-ranged (for the correct explanation please see the note at page 2 in [8]), which means that distant particles are not interacting in any way. Mathematically, these systems may be identified as quasi-Poissonian and it can then be proven rigorously (as is in A.1) that associated headway distributions necessarily belong to class \mathcal{B} of balanced distribution [8,18,9]. Therefore any socio-physical headway distribution fulfills the criteria for balanced distribution. A probability density function $g(x)$ is called *balanced* if there exists $\omega > 0$ so that

$$\forall x \in (0, \omega) : \lim_{x \rightarrow +\infty} g(x)e^{xx} = 0, \quad (5)$$

and

$$\forall x > \omega : \lim_{x \rightarrow +\infty} g(x)e^{xx} = +\infty. \quad (6)$$

The number ω is then called *the balancing index* and denoted by $\text{inb}(g)$. Representatives of the set \mathcal{B} are, for example, exponential distribution, Erlang distribution, Gamma distribution, and generalized inverse Gaussian distribution. Contrariwise, log-normal distribution or normal distribution does not belong to \mathcal{B} .

To conclude, theoretically-based predictions for socio-physical headway distributions should show a balanced tail. This is, as justified above, a general property of all quasi-Poissonian ensembles. Therefore, any proposal for functions estimating empirical headway distributions in traffic/pedestrian systems must comply with the above-mentioned criterion (*the balancing criterion*).

4. Scenarios of experiments and description of empirical measurements

The study presented is based on four independent data collections: three experimental and one empirical. Although some measurements were not primarily designed for the time headway studies, the layout of the monitored areas and recording methods allowed to collect the time headway data according to the above mentioned restrictions, i.e., unidirectional, one-lane flow without overtaking. It is worth noting that the one-lane non-overtaking flow was achieved by different means: It was not possible in the passing-through experiment and Kretz bottleneck experiment due to the narrow corridor. It was forbidden in the following-walkers experiment. It was extremely rare in the shopping center observation due to quite narrow corridor and social conventions. The detailed description of all scenarios follows below.

4.1. The passing-through experiment

The passing-through experiment was set up in April 2014 at the Czech Technical University in Prague (Faculty of Nuclear Sciences and Physical Engineering) with 75 students acting as pedestrians. The experiment was designed for a boundary-induced phase transition study (details in [16]); pedestrians were passing through a small room with an exit 60 cm wide, followed by a corridor of the same width. They were not supposed to simulate panic-like behavior. Despite that, their motivation to leave the room as fast as possible was quite high, because the crowd assembled before the bottleneck was rather large, i.e. up to 5 pedestrians per square meter.

For the purposes of the article we use the time headways measured at three spots of the outflow corridor: directly at the exit (Detector 1), 1 m downstream from the exit (Detector 2), and 2 m downstream from the exit (Detector 3). As shown below, the bottleneck acts like a synchronization element because in the corridor (downstream from the exit) the territorial social force prevails against the acceleration force pushing pedestrian towards and through the exit in order that they may escape the uncomfortable zone.

This experiment is further referred to as First, Second, and Third Detector.

4.2. The following-walkers experiment (walkers on the line)

The following-walkers experiment was performed in January 2015 at the Brno University of Technology (Faculty of Civil Engineering). Twenty two pedestrians were instructed to walk in a linear formation, each pedestrian following their predecessor. It means that pedestrians walked in a line, following the leader, who was choosing the path. Time headways have been extracted from the video records at a given cross-section. From the essence of the experiment it is obvious that motivation of pedestrians to move forward was lower than in the passing-through experiment. Therefore, the level of synchronization was higher because the territorial social force dominated over the acceleration term.

This experiment is further referred to as Walkers on the line.

4.3. Shopping center observation

The data observed empirically have been provided by Pavel Křiváň, who recorded the flow in a shopping center in Pardubice. Operators of the center built corridors in the lobby due to reconstructions underway in the central part of the lobby. Furthermore, the visitors were instructed to choose the given corridor for the given direction of motion and follow the one-way signs. This situation was recorded for several days. Nevertheless, for the purpose of this article, only rush hours records have been used in order to assure constant flow of pedestrians, which motivated the visitors to keep the ordered walking direction. To eliminate the influence of pedestrians entering or leaving the pedestrian stream, a virtual detector for time headway measurements was placed at a significant distance from entrances to individual shops.

This observation is further referred to as Empirical Headways.

4.4. Pedestrian flows through a bottleneck

The fourth data sample was provided by Tobias Kretz. The flow through bottlenecks of various width has been studied in [26] in order to provide a dependence between the bottleneck width and pedestrian flow through it. This article makes use of data related only to flow through bottlenecks 40, 50, and 60 cm in width.

This experiment is further referred to as Kretz et al.

4.5. Data processing

Previously mentioned experiments have been recorded on camera. The video footage has been processed automatically using image recognition techniques (First–Third Detector) or manually (Walkers on the line, Empirical Headways, Kretz et al.). For further analysis, the time series $(t_j)_{j=0}^N$ of crossings of certain virtual detector have been used. For each run of the experiment, the crossing times have been transformed to sequences of scaled time headways $(\tau_j)_{j=0}^N$ (see Eq. (1) and discussion below). The scaling to mean value equal to one enables the comparison of the interaction essence in different data samples.

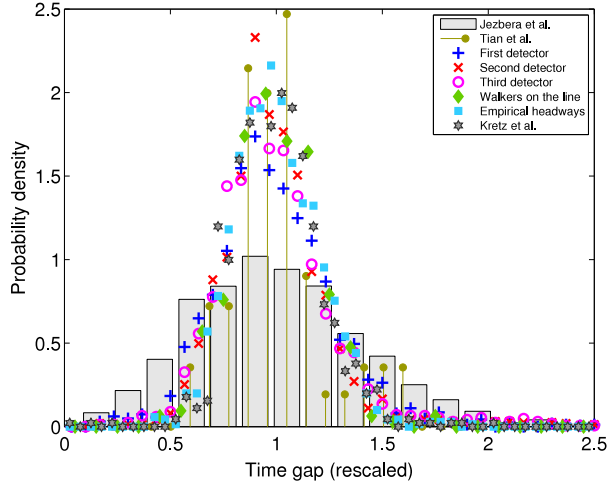


Fig. 1. The experimental/empirical headway distributions. The signs represent the probability density of scaled time gaps among neighboring walkers passing a detector. As announced in the legend, the bars, stems, and hexagrams correspond to researches published in [14,15,26], respectively. The other signs display headway distributions analyzed from original experiments presented in this paper. Analogous trends in headway distribution has been also detected in [10].

The scaled sequences (for given experiment) have been aggregated to one sequence, which was used for further statistical analysis (headway distribution, spectral rigidity). This procedure is justified by the assumption that the successive headways can be considered as independent. This is discussed in more detail in Section 8. This procedure enabled to gain sufficient amount of information even from experiments with low number of pedestrians and low number of records in individual runs of the experiment.

A preliminary analysis of THD is visualized in Fig. 1. Besides headways gauged especially for this paper we also plot (for illustration) THD analyzed from previous researches published in [14,15,26]. It is of note to point to the incompatibility between the histogram (shown in Fig. 1) plotted for data obtained by Jezbera et al. [14] and histograms plotted for other sources. According to the authors of the article [14], this conspicuous discrepancy can be attributed to an inaccurate measurement method.

5. Analytical estimations of territorial social forces

Following the general strategy presented in Section 2, we intend to examine elementary estimations – if any – for territorial social forces $f(s)$ for which the analytically-determined headway distributions correspond to empirical/experimental histogram functions. Actually, attempts to estimate the force action are not entirely new. In the articles [26,10,3,11] their authors investigate either headway distribution or suggest statistical distribution models or suggest distance dependence of the interaction forces. On the contrary, our paper presents a theoretically-substantiated link between territorial social forces and distribution of time gaps.

First, we suggest (with respect to the previous considerations) two natural choices for a force description: logarithmic and hyperbolic potential. The logarithmic potential $\varphi(s) = -\log(s)$ corresponds to repulsion decreasing with the distance according to $f(s) = s^{-1}$. The corresponding quantities are further marked with subscript L. The hyperbolic potential $\varphi(s) = s^{-1}$ results in a stronger repulsion force $f(s) = s^{-2}$. The corresponding quantities are marked with subscript H. The associated headway distributions read

$$\wp_L(\tau|\beta) = \Theta(\tau) \frac{(\beta + 1)^{\beta+1}}{\Gamma(\beta + 1)} \tau^\beta e^{-(\beta+1)\tau}; \tag{7}$$

$$\wp_H(\tau|\beta) = A\Theta(\tau) e^{-\frac{\beta}{\tau} - D\tau}; \tag{8}$$

where

$$D = \beta + \frac{3 - e^{-\sqrt{\beta}}}{2}; \quad A^{-1} = 2\sqrt{\frac{\beta}{D}} \mathcal{K}_1(2\sqrt{D\beta}).$$

Here $\mathcal{K}_1(x)$ stands for Macdonald’s function of the first order. Note that both distributions belong to the family of balanced distributions discussed in Section 3. We remark that distribution (7) has already been found in [10] being a suitable candidate for a time headway distribution of pedestrian groups.

Table 1
Quantitative summary of pedestrian experiments and minimum distance estimations.

Detector	Number of headways	Average headway [ms]	$\hat{\beta}_L$	$\hat{\beta}_H$	$\tilde{\varrho}(\hat{\beta}_L)$	$\tilde{\varrho}(\hat{\beta}_H)$
First detector	2452	739	13.870	6.513	0.06278	0.06365
Second detector	2440	745	21.817	10.431	0.11439	0.10040
Third detector	2531	761	17.014	8.017	0.10223	0.08287
Walkers on the line	316	708	23.652	11.459	0.03909	0.05532
Empirical headways	1406	858	23.555	11.373	0.02016	0.03786
Kretz et al.	901	1140/980/870	27.550	13.279	0.03739	0.03325

Practically, in Fig. 2 the PDFs (7) and (8) are plotted against the empirically/experimentally obtained data of time headways. Parameter β of the considered distribution families has been estimated by means of the minimum-distance estimation method using distance

$$\tilde{\varrho}(\beta) := \left(\int_0^\infty \left(\int_0^x (\varphi(\tau|\beta)) - H(\tau|\Delta_\tau) d\tau \right)^2 dx \right)^{1/2}, \tag{9}$$

i.e., $\hat{\beta} = \operatorname{argmin}_{\beta \in [0, \infty)} \tilde{\varrho}(\beta)$. In Fig. 2 it is evident that the empirical/experimental headways are very convincingly described by both approximations (see also Table 1). In fact (as seen if comparing the last two columns in Table 1 and if calculating distance ϱ between both estimations), it is hard to distinguish between the approaches proposed because both curves (calibrated to data) are extremely close. A smaller amount of data precludes recognition of more detailed nuances in THD. Therefore, the THD analysis seems to be insufficient to make a decision between logarithmic and hyperbolic potentials.

6. Statistical rigidity and compressibility

Although analyzing and estimating headway distributions is a natural way to inspect the microstructure of pedestrian crowds, the formal background of such investigations is disputable. Measurements, data processing, and automatic evaluation techniques are burdened by systematic errors and extensive inaccuracies. Therefore, we search for any logical alternative which should be (a) directly measurable; (b) less prone to inaccuracies; (c) mathematically well-established. So a natural candidate then seems to be statistical rigidity defined/studied in [6–8,14,23,17]. In pedestrian dynamics statistical rigidity represents (formally speaking) a variance of pedestrian flux (see also [14]). Obviously, pedestrian flux is understood to be the number of pedestrians passing any fixed point during a given time interval. Therefore, the fundamental quantity for flux enumeration is a random variable $N(T)$ representing number of pedestrians crossing a detector during a time interval T . Statistical nature of $N(T)$ generates fluctuations of individual realizations of $N(T)$. They are standardly described by a quantity called statistical rigidity defined by

$$\Delta(T) = \sum_{k=0}^\infty (k - T)^2 \mathbb{P}[N(T) = k], \tag{10}$$

where $\mathbb{P}[N(T) = k]$ stands for probability that number of pedestrians detected during T is exactly equal to k . We also add that $\langle N(T) \rangle = T$, which is because the mean headway (as explained in the previous sections) is strictly set to one. Formula (10) represents a pseudo-variance of $N(T)$ around the average value $\langle N(T) \rangle$. Since in the particles/agents interaction systems condition $\langle N(T) \rangle = \mathbb{E}(N(T))$ is not usually met, the quantity (10) is not a standard variance. For systems with uncorrelated subsequent headways (see also Section 8) there exists (see [8]) a direct link between headway distribution (or its Laplace image $G(s) = \mathfrak{L}[g]$) and rigidity. According to A.2, it holds that

$$\mathfrak{L}[\Delta(T)] = \frac{2}{s^3} + \frac{(s - 2)G(s) + 2sG'(s) + (s + 2)G^2(s)}{s^2(G(s) - 1)^2}. \tag{11}$$

According to [6,23,8], the rigidity satisfies a condition $\Delta(T) = \chi T + \mu + \mathcal{O}(T^{-1})$, and, therefore, it can be (extremely accurately) approximated by the linear function $\Delta(T) \approx \chi T + \mu$ for $T \gg 0$. For both above-mentioned headway distributions the relevant asymptotical behavior has been derived in [8,6]. It holds (after applying (11)) that

$$\Delta_L(T) \approx \frac{T}{\beta + 1} + \frac{\beta(\beta + 2)}{6(\beta + 1)^2}; \tag{12}$$

$$\Delta_H(T) \approx \frac{2 + \sqrt{D\beta}}{2D(1 + \sqrt{D\beta})} T + \frac{6\sqrt{D\beta} + D\beta(21 + 4D\beta + 16\sqrt{D\beta})}{24(1 + \sqrt{D\beta})^4}. \tag{13}$$

Slope χ of this linear asymptote is usually referred to as compressibility, whose specific value (lying between 0 and 1) corresponds to the level of synchronization between mutual positions of elements (pedestrians, vehicles). For systems, where interactions between agents are weak, one can expect a low level of synchronization, i.e. $\chi \approx 1$. However, if the

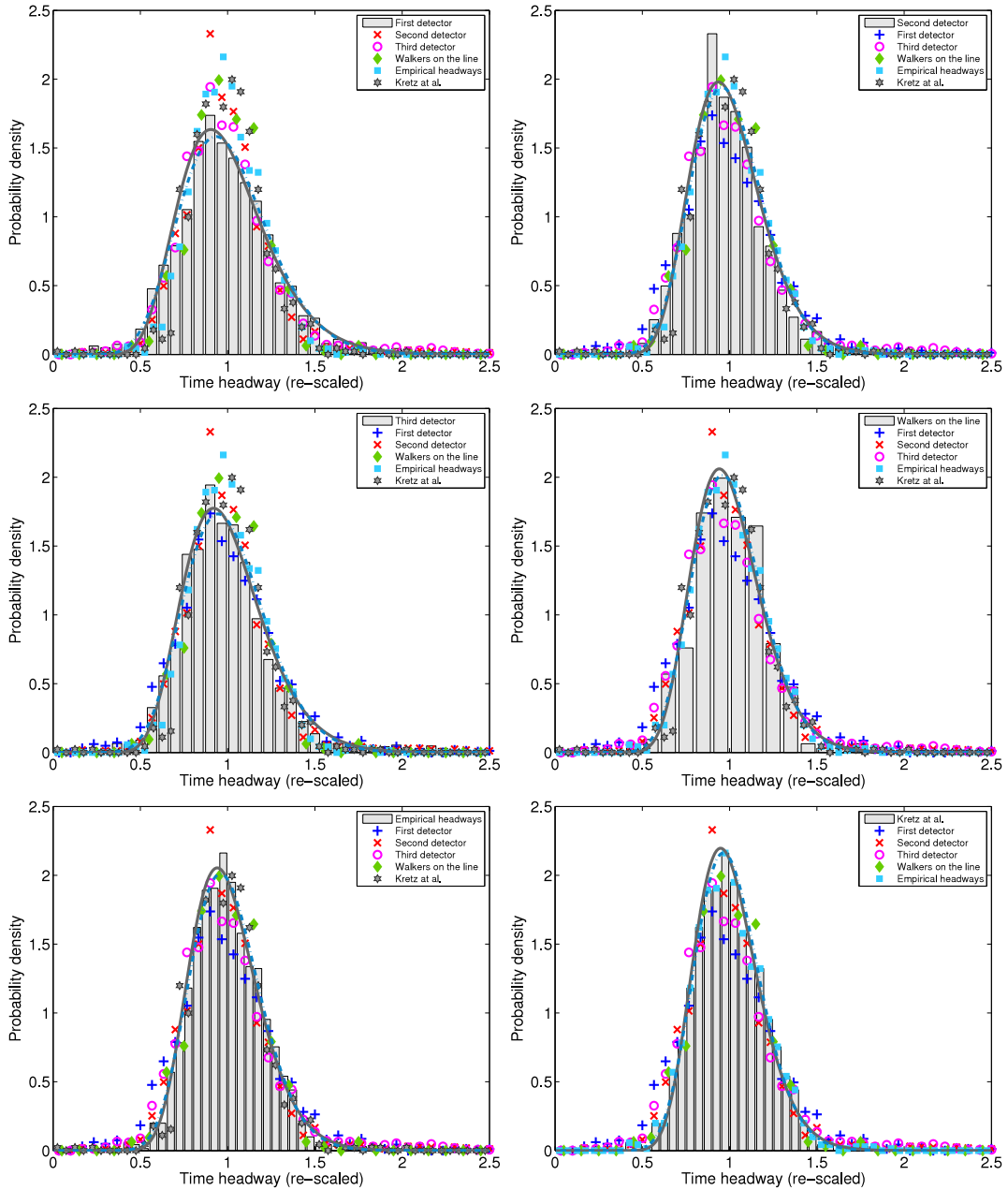


Fig. 2. Analytical estimations of empirical/experimental headway distributions. Black curve visualizes a graph of the function (8) enumerated for the parameter $\hat{\beta}_H$ estimated by MDE (see Table 1). Blue (dash-dotted) curve displays a course of the theoretical prediction (7) with the estimated parameter $\hat{\beta}_L$. Histograms represent distributions subjected to estimations (see legend). Signs (showing headway distributions measured for rest experiments – see Fig. 1) are drawn for clarity.

agent's interactions are more intensive, the level of synchronization increases and, therefore, compressibility decreases. The rigidity analysis applied to all data sources available is shown in Fig. 3. The graphical outputs show interesting distinctions between various pedestrian data as well as distinctions between vehicular and pedestrian traffic. In some of the investigated systems (shopping center data, Kretz data) compressibility is rapidly subdued, which corresponds to a stronger force action and/or lower level of randomness between walkers.

Moreover, Fig. 3 provides an interesting comparison between pedestrian and vehicular streams. Although the basic interaction principles are the same in both systems, different levels of fluctuations are responsible for significantly different values of compressibility. At first sight, this is a surprising finding because a wrong maneuver of a driver has much more serious consequences than of a walker. Therefore, one can expect increased vigilance of drivers, which intuitively should

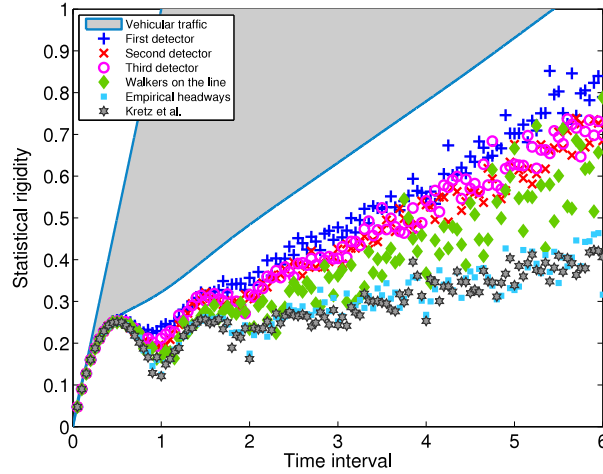


Fig. 3. Statistical rigidity in empirical/experimental data. Graphs of the statistical rigidity analyzed for all available pedestrian data (see legend for details). The gray zone shows a region of vehicular rigidities, i.e. empirical statistical rigidity detected for vehicular traffic is usually (according to [6,8,7,23]) a curve lying in this zone.

lead to a more systematic arrangement of vehicles. However, this study definitely refutes such behavior. Since, however, compressibility χ is strictly decreasing with resistivity β Fig. 3 demonstrates that pedestrian systems (contrary to vehicular systems) are much more resistant to statistical fluctuations, which means that ensembles of walkers are substantially closer to deterministic systems than vehicular systems. This observation can be explained by the fact that maneuvering of drivers is, as expected, much more variable than the maneuvering of walkers, which is due to a larger variance of speeds. Also, driving a vehicle is not so natural for humans as ordinary walking.

7. Compressibility-based estimations

Owing to the fact that tests of statistical rigidity are, without any doubt, more compelling (not burdened by inaccuracies) than those using headways, we use statistical rigidity as the main instrument for making a decision which potentials (logarithmic/hyperbolic) or balanced distributions (7)/(8) are more suitable for statistical description of crowd microstructure. Thus, estimating the compressibility of pedestrian data (using simple linear regression applied to linear tails in graphs of statistical rigidity) we calculate values

$$\hat{\beta}_L = \frac{1}{\chi} - 1, \tag{14}$$

$$\hat{\beta}_H = \hat{\beta}_H(\chi) \quad \& \quad 2 + \sqrt{\hat{\beta}_H D(\hat{\beta}_H)} = 2\chi D(\hat{\beta}_H) \left(1 + \sqrt{\hat{\beta}_H D(\hat{\beta}_H)} \right) \tag{15}$$

of estimated values $\hat{\beta}_L$ and $\hat{\beta}_H$ for both potentials. Knowing $\hat{\beta}_L$, $\hat{\beta}_H$ we then calculate the statistical distance

$$\varrho_{L/H} := \left(\int_0^\infty \left(\int_0^x (\wp(y|\hat{\beta}_{L/H}) - H(y|\Delta_\tau)) dy \right)^2 dx \right)^{1/2} \tag{16}$$

between the estimated theoretical distribution and empirical/experimental time headway distribution. Values ϱ_L and ϱ_H (expressed for six data sources) can then be used for final decision which of the two considered potentials (or distribution models) is more suitable for theoretical estimations of territorial social interactions acting inside a group of moving individuals.

As quantified in Table 2 in all cases (except for shopping center observations) the statistical distance ϱ_L (assuming gamma-distributed headways) is greater than ϱ_H (assuming GIG-distributed headways). It seems therefore that force description based on hyperbolic repulsions is closer to reality than the description using a logarithmic potential. The same conclusion has been drawn (in [4,7,8]) for vehicular streams as well. Relatively high values of these distances confirm the expected premise that statistical analysis of pedestrian headways is less informative, which is a logical consequence of the fact that digital processing (automatic detection) of gaps between walkers is quite inaccurate. On the other hand, calculations of statistical rigidity (based on counting walkers passing by a given point at a given time interval) are more accurate, by an order of magnitude.

Table 2
Summary of compressibility-based estimations.

Detector	χ	$\hat{\beta}_L$	$\hat{\beta}_H$	ϱ_L	ϱ_H	α
D1	0.1180	7.4750	3.5473	0.20059	0.18686	0.019276
D2	0.0978	9.2203	4.4450	0.26470	0.24165	0.005719
D3	0.1025	8.7557	4.2051	0.21349	0.18862	0.010649
Line	0.0974	9.2647	4.4665	0.26762	0.26005	0.057904
SC	0.0437	21.8608	10.8514	0.03940	0.04497	0.002478
Kretz	0.0441	21.6779	10.7469	0.09035	0.07993	0.011544

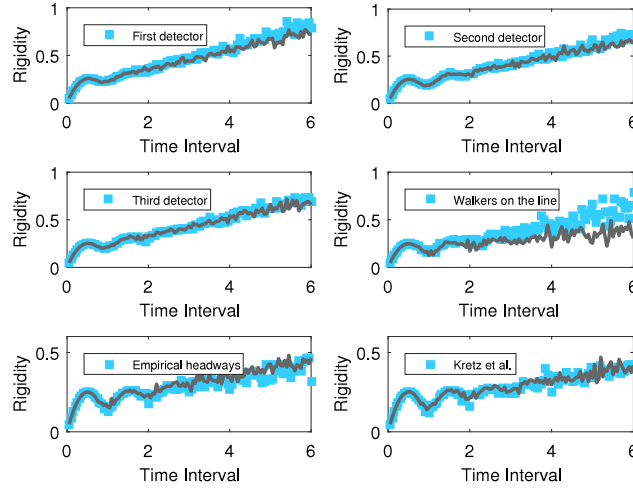


Fig. 4. Test of a statistical independence of successive headways. We plot the statistical rigidity calculated for individual data sources (squares) against the rigidity analyzed for sets of the randomly shuffled headways (line).

8. Assumption of statistical independence for headways

Note that all the previous considerations (i.e. predominantly analytical derivations for statistical rigidity) are valid only under the assumption that the neighboring spacings are independent. Therefore, it is essential (for practical applications) to test whether such a premise is reasonable or not. Thus, we test if statistical rigidity of the analyzed data sources is or is not influenced by random changes of the order of headways. Since randomly shuffled headways (analyzed for systems with short- or middle-ranged cooperation) are, without any doubt, independent, Fig. 4 confirms the legitimate use of the above-mentioned approaches. A slight deviation is detected for walkers on the line, which is caused by insufficient length of data sample (compare the numbers in the second column of Table 1).

To be specific, let us consider vector $\vec{\tau} = (\tau_1, \tau_2, \dots, \tau_N)$ of successive headways arranged in the original order (chronologically with respect to the time of measurement). Let π be a randomly generated permutation of $\{1, 2, \dots, N\}$. Then $\vec{\chi} = (\chi_1, \chi_2, \dots, \chi_N) := (\tau_{\pi(1)}, \tau_{\pi(2)}, \dots, \tau_{\pi(N)})$ is the vector of randomly shuffled headways, where all statistical links between successive headways χ_k, χ_{k+1} have been broken by the afore-mentioned randomization. It is well known (from Random Matrix Theory) that vectors of dependent headways show a significant deviation from the formula derived for independent headways. Therefore, an angular deviation between linear asymptotes $\chi_{\vec{\tau}} T + \mu_{\vec{\tau}} \approx \Delta_{\vec{\tau}}$ and $\chi_{\vec{\chi}} T + \mu_{\vec{\chi}} \approx \Delta_{\vec{\chi}}$ reflects a certain measure of dependence in $\vec{\tau}$. Practically, such deviation can be quantified by

$$\alpha = |\chi_{\vec{\tau}} - \chi_{\vec{\chi}}|. \quad (17)$$

If $\alpha > \alpha_0$, where α_0 is a normal deviation (here we consider $\alpha_0 \approx 0.02$); then the detected deviation is statistically significant and the analyzed headways can be classified as dependent. The last column of Table 2 summarizes numerical outputs of the method proposed.

9. Conclusions

This article reports on several pedestrian experiments (original or reproduced) proposed for analyzing a microstructure of a group of walkers moving unidirectionally in a narrow corridor. At first, we have shown that statistical distribution of time gaps between neighboring pedestrians can be convincingly described by some probability density belonging to a family of balanced distributions (e.g. gamma distribution or GIG distribution). This knowledge generalizes the recent results published in [10], and, in practice, it can be used for quantitative assessments of pedestrian models or for predictions of corridor capacities.

By introducing a stochastic force-based scheme (controlled by coefficient of statistical resistivity β) we relate the detected headway distribution with the associated force description. In other words, we estimate the territorial social forces (and their dependence on distances between walkers) by making the use of knowledge of spatiotemporal arrangement of individuals in pedestrian groups.

Useful information about the statistical nature of systems investigated is obtained by calculation of coefficient β quantifying measure of statistical resistivity, i.e. measuring the nearness to deterministic arrangement of pedestrian locations.

A deeper insight into the pedestrian flow microstructure is made possible by a thorough analysis of statistical rigidity. The efficiency of an instrument of statistical rigidity is apparent when comparing the compressibility among all systems observed. Indeed, although the time headway distributions in all systems are relatively close, a course of the rigidity reveals mutual nuances. They are caused by different levels of compressibility. As far as the passing-through experiment is concerned, Fig. 3 shows that compressibility χ depends on the location of the detector, which indicates changes in pedestrian synchronization in the course of time. This supports the idea that with time pedestrian headways evolve so that compressibility decreases. The level of synchronization for walkers in a line in a free area is visibly larger than in corridors with a boundary. Stronger synchronization is detected for empirical flows measured in a narrow corridor and for passage through a door.

Both methods, however, suffer from relatively inaccurate detection of time gaps between individuals, which is a well-known problem of crowd modeling.

Moreover, new interesting knowledge has been obtained by comparing of compressibility between vehicular and pedestrian streams. It follows from Fig. 3 that synchronization of walkers is much more intensive than that of cars. The effect is the same for statistical resistivity. Such difference is given by the fact that vehicular flows allow (due to larger variances of speed) a greater fluctuation level than pedestrian flows. Thus, the suggested approach allows to differentiate between various agent's systems using a set of headways only, which is a great benefit.

From the practical point of view, the suggested methodology based on tests of statistical rigidity seems to be a suitable instrument for theoretical validations of various pedestrian models. The low values of compressibility reveals that the repulsion force between pedestrians has hard-core-like nature. This should be taken into account in model formulation, which means that the potential generated by the model agent should be very high in the close neighborhood of the agents and should vanish very fast with distance to the agent. The compressibility value could be then used for proper parameters calibration.

Acknowledgments

The authors would like to thank Tobias Kretz for providing original pedestrian data (originally published in [26]), Pavel Křiváň for recording and analyzing shopping center data, and Faculty of Civil Engineering, Brno University Of Technology for arranging several pedestrian experiments used in this article.

The research presented in this work was supported by Grant 15-15049S of Czech Science Foundation (GA ČR). Partial support was provided by the Czech Technical University in Prague within the internal project SGS15/214/OHK4/3T/14.

Appendix

A.1. Quasi-Poissonian ensembles and class of balanced distributions

As is generally known, particle system is called *Poissonian* if probability $\mathbb{P}[N_L = k]$ (i.e. probability that number of particles lying inside a interval of length L is equal to k) reads

$$\mathbb{P}[N_L = k] = \frac{(\lambda L)^k}{k!} e^{-\lambda L}, \quad (18)$$

where $\lambda > 0$ is a parameter. On the other hand, particle system is called *quasi-Poissonian* if

$$(\exists \lambda \in \mathbf{R}^+)(\forall \epsilon > 0)(\exists L_\epsilon \in \mathbf{R}^+) : k \in \mathbf{N} \wedge L > L_\epsilon \Rightarrow \left| \mathbb{P}[N_L = k] - \frac{(\lambda L)^k}{k!} e^{-\lambda L} \right| < \epsilon. \quad (19)$$

This definition can be less formally interpreted as a fact that on a large scale (for large distances) particles of a quasi-Poissonian system are distributed like those of a certain Poissonian system. Since a relation between a headway distribution $g(x)$ and probability $\mathbb{P}[N_L = k]$ is described by the formula

$$g(x) = - \frac{d\mathbb{P}[N_x = 0]}{dx} \quad (20)$$

we conveniently use the definition (19) with $k = 0$. Thus,

$$1 - \epsilon - e^{-\lambda x} < 1 - \mathbb{P}[N_x = 0] < 1 + \epsilon - e^{-\lambda x}, \quad (21)$$

where $G(x) := 1 - \mathbb{P}[N_x = 0]$ is in fact a distribution function for $g(x)$, i.e. $g(x) = \lim_{\tau \rightarrow 0} \frac{G(x+\tau) - G(x)}{\tau}$. After simple modifications of (21) we have

$$-\frac{2\epsilon + e^{-\lambda(x+\tau)} - e^{-\lambda x}}{\tau} < \frac{G(x+\tau) - G(x)}{\tau} < \frac{2\epsilon - (e^{-\lambda(x+\tau)} - e^{-\lambda x})}{\tau}. \quad (22)$$

Therefore (for $\mu < \lambda$, $\epsilon = \tau^2$, and $\tau \rightarrow 0$)

$$g(x)e^{\mu x} \leq \frac{2\epsilon e^{\mu x} - (e^{-\lambda(x+\tau)} - e^{-\lambda x})e^{\mu x}}{\tau}, \quad (23)$$

hence

$$0 \leq \lim_{x \rightarrow +\infty} g(x)e^{\mu x} \leq - \lim_{x \rightarrow +\infty} e^{\mu x} \lim_{\tau \rightarrow 0} \frac{e^{-\lambda(x+\tau)} - e^{-\lambda x}}{\tau} = \lim_{x \rightarrow +\infty} e^{\mu x} \lambda e^{-\lambda x} = 0. \quad (24)$$

Thus, $\lim_{x \rightarrow +\infty} g(x)e^{\mu x} = 0$, which completes the first part (5) of the definition of balanced probabilities. Analogously, for $\mu > \lambda$ one can obtain

$$\frac{-2\epsilon e^{\mu x} - (e^{-\lambda(x+\tau)} - e^{-\lambda x})e^{\mu x}}{\tau} \leq g(x)e^{\mu x} \quad (25)$$

and $e^{\mu x} \lambda e^{-\lambda x} \leq g(x)e^{\mu x}$. Since $\lim_{x \rightarrow +\infty} \lambda e^{(\mu-\lambda)x} = +\infty$ we see that also $\lim_{x \rightarrow +\infty} g(x)e^{\mu x} = +\infty$, which completes the second part (6) of the definition of balanced probabilities. As a summary: $g(x) \in \mathcal{B}$ and $\text{inb}(g) = \lambda$.

A.2. Laplace image of the statistical rigidity

Consider now an arbitrary one-dimensional particle system in which the mean headway is fixed to 1. Let random variable N_L represent a number of particles locating inside an interval $[0, L]$. It is well known (see [6,8]) that the expected value for N_L is

$$\mathbb{E}[N_L] = \int_0^L \mathcal{R}(x) dx, \quad (26)$$

where $\mathcal{R}(x) = \sum_{k=0}^{\infty} \wp_k(x)$ is the cluster function and $\wp_k(x)$ is the probability density for a mutual distance between $k + 2$ successive particles. The latter can be (if successive headways are not correlated) calculated by means of a convolution rule $\wp_k(x) = \star_{n=0}^k \wp(x)$, where $\wp(x) \equiv \wp_0(x)$ is the headway distribution (probability density for a gap between immediately adjacent particles). The statistical rigidity $\Delta(L) := \sum_{k=0}^{\infty} (k - L)^2 \mathbb{P}[N_L = k]$ can be rewritten as

$$\Delta(L) = \mathbb{E}[N_L^2] - 2L\mathbb{E}[N_L] + L^2. \quad (27)$$

That leads (after using the relation $\sum_{k=0}^{\infty} k \wp_k(x) = \mathcal{R}(x) \star \mathcal{R}(x)$) to the simplified version

$$\Delta(L) = 2\mathcal{R}(L) \star \mathbb{E}[N_L] + \mathbb{E}[N_L] - 2L\mathbb{E}[N_L] + L^2. \quad (28)$$

Furthermore, following general properties of Laplace transformation one can easily show that the Laplace image of the cluster function reads

$$R(s) = \mathcal{L}[\mathcal{R}(x)] = \frac{\mathcal{L}[\wp(x)]}{1 - \mathcal{L}[\wp(x)]}. \quad (29)$$

With help of these considerations we can modify the relation (28) to the final shape

$$s^3 \mathcal{L}[\Delta(L)] = 2 + s \frac{(s-2)P(s) + 2sP'(s) + (s+2)P^2(s)}{(P(s) - 1)^2}, \quad (30)$$

which express a direct dependence between the Laplace image of the rigidity and Laplace image $P(s) = \mathcal{L}[\wp(x)]$ of the headway distribution.

References

- [1] A. Schadschneider, W. Klingsch, H. Klüpfel, T. Kretz, Ch. Rogsch, A. Seyfried, *Evacuation Dynamics: Empirical Results, Modeling and Applications, Extreme Environmental Events: Complexity in Forecasting and Early Warning*, Springer, New York, 2011.
- [2] A. Schadschneider, D. Chowdhury, K. Nishinari, *Stochastic Transport in Complex Systems*, Elsevier, 2010.
- [3] D. Helbing, A. Johansson, Pedestrian, crowd and evacuation dynamics, in: *Encyclopedia of Complexity and Systems Science*, Springer, Heidelberg, 2009.
- [4] M. Krbálek, D. Helbing, Determination of interaction potentials in freeway traffic from steady-state statistics, *Physica A* 333 (2004) 370–378.
- [5] M. Krbálek, Equilibrium distributions in a thermodynamical traffic gas, *J. Phys. A* 40 (2007) 5813–5821.
- [6] M. Krbálek, P. Šeba, Spectral rigidity of vehicular streams (random matrix theory approach), *J. Phys. A* 42 (2009) 345001/1–10.
- [7] M. Krbálek, Inter-vehicle gap statistics on signal-controlled crossroads, *J. Phys. A* 41 (20) (2008).
- [8] M. Krbálek, J. Šleis, Vehicular headways on signalized intersections: theory, models, and reality, *J. Phys. A* 48 (2015) 015101/1–22.

- [9] M. Krbálek, Theoretical predictions for vehicular headways and their clusters, *J. Phys. A* 46 (2013) 4451011/1–19.
- [10] N.W.F. Bode, E.A. Codling, Statistical models for pedestrian behaviour in front of bottlenecks, in: V.L. Knoop, W. Daamen (Eds.), *Traffic and Granular Flow '15*, Springer International Publishing, 2016, pp. 81–88.
- [11] A. Johansson, D. Helbing, P.K. Shukla, Specification of the social force pedestrian model by evolutionary adjustment to video tracking data, *Adv. Complex Syst.* 10 (2007) 271–288.
- [12] D. Helbing, I. Farkas, T. Vicsek, Simulating dynamical features of escape panic, *Nature* 407 (6803) (2000) 487–490.
- [13] D. Helbing, P. Molnár, Social force model for pedestrian dynamics, *Phys. Rev. E* 51 (5) (1995) 4282–4286.
- [14] D. Jezbera, D. Kordek, J. Kříž, P. Šeba, P. Šroll, Walkers on the circle, *J. Stat. Mech.* (2010) L01001/1–10.
- [15] W. Tian, W.G. Song, J. Ma, Z. Fang, A. Seyfried, J. Liddle, Experimental study of pedestrian behaviors in a corridor based on digital image processing, *Fire Saf. J.* 47 (2012) 8–15.
- [16] M. Bukáček, P. Hrabák, M. Krbálek, Experimental study of phase transition in pedestrian flow, *Transp. Res. Proc.* 2 (2014) 105–113.
- [17] M.L. Mehta, *Random Matrices*, third ed., Academic Press, New York, 2004.
- [18] M. Krbálek, T. Hobza, Inner structure of vehicular ensembles and random matrix theory, *Phys. Lett. A* 380 (21) (2016) 1839–1847.
- [19] M. Krbálek, P. Šeba, Statistical properties of the city transport in Cuernavaca (Mexico) and random matrix ensembles, *J. Phys. A: Math. Gen.* 33 (2000) L229–L233.
- [20] M. Krbálek, P. Šeba, Headway statistics of public transport in Mexican cities, *J. Phys. A: Math. Gen.* 36 (2003) L1–L5.
- [21] J. Baik, A. Borodin, P. Deift, T. Suidan, *J. Phys. A: Math. Gen.* 39 (2006) 8965–8975.
- [22] A.E. Schefflen, N. Ashcraft, *Human Territories: How We Behave in Space-Time*, Prentice-Hall, Englewood Cliffs, 1976.
- [23] M. Krbálek, Analytical derivation of time spectral rigidity for thermodynamic traffic gas, *Kybernetika* 46 (6) (2010) 1108–1121.
- [24] M. Treiber, D. Helbing, Hamilton-like statistics in onedimensional driven dissipative many-particle systems, *Eur. Phys. J. B* 68 (2009) 607–618.
- [25] L. Li, X.M. Chen, Vehicle headway modeling and its inferences in macroscopic/microscopic traffic flow theory: A survey, *Transp. Res. C* 76 (2011) 170–188.
- [26] T. Kretz, A. Grünebohm, M. Schreckenberg, Experimental study of pedestrian flow through a bottleneck, *J. Stat. Mech.* (2006) P10014/1–20.
- [27] A. Seyfried, O. Passon, B. Steffen, M. Boltes, T. Rupperecht, New insights into pedestrian flow through bottlenecks, *Transp. Sci.* 43 (3) (2009) 395–406.
- [28] W. Liao, A. Tordeux, A. Seyfried, M. Chraïbi, K. Drzycimski, X. Zheng, Y. Zhao, Measuring the steady state of pedestrian flow in bottleneck experiments, *Physica A* 461 (2016) 248–261.